A Sensing Framework for Indoor Spatial Awareness for Blind and Visually Impaired Users

Zhuorui Yang, Student Member, IEEE, and Aura Ganz, Fellow, IEEE

Abstract—In this paper, we present a Bluetooth Low Energy (BLE)-based sensing framework that provides real time spatial awareness for blind and visually impaired (BVI) users while navigating independently through large public venues. The proposed framework includes the following functionalities using only the Received Signal Strength Indicator (RSSI) obtained from the BLE sensors: 1) determining the location of the user, 2) estimating user's moving direction, and 3) detecting proximity of landmarks next to the user. We evaluate these functionalities individually. Moreover, we incorporate the proposed framework in PERCEPT indoor navigation system and test it with BVI users in a large public venue. Testing results show that the location, moving direction and landmark proximity computed by the framework, although not very accurate, provide sufficient information to enable BVI users to independently navigate in large indoor venues. This conclusion aligns with Nobel Prize winning findings that confirm the spatial nature of the entorhinal-hippocampal system and the existence of a positioning system in the brain.

Index Terms—Indoor Localization, Bluetooth Low Energy, Sensing Framework, Spatial Cognition, Cognitive Neuroscience, Visually Impaired.

I. INTRODUCTION

Traveling independently in unfamiliar large public venues is a very challenging task for blind and visually impaired (BVI) people [1]. In [2-4] we introduced PERCEPT indoor navigation system for BVI users which enables them to independently navigate in large indoor spaces. In this paper we introduce a sensing framework which was integrated and successfully tested in PERCEPT system. The framework provides user location, moving direction and proximity to landmarks.

In cognitive neuroscience, there is a consensus [5] that one's ability of navigation depends on one's capability to build the cognitive map of the space. Using this map, humans can position and navigate themselves inside the space. To identify the needs of humans in spatial positioning and navigation and develop corresponding navigation aids, it is necessary to know how the brain encodes the space from a neuroscientific viewpoint [6]. There are four types of cells found in the spatial representation in the brain (see Fig. 1).

1. **Place cells (Fig. 1a)** are pyramidal neurons inside the hippocampus which fire when an individual (animal or human) visits a particular place (small region) in the environment, thereby exhibiting a representation of the place with respect to the environment [7]. This area of high firing rate is known

Department of Electrical and Computer Engineering, University of Massachusetts, Amherst, MA 01002 USA

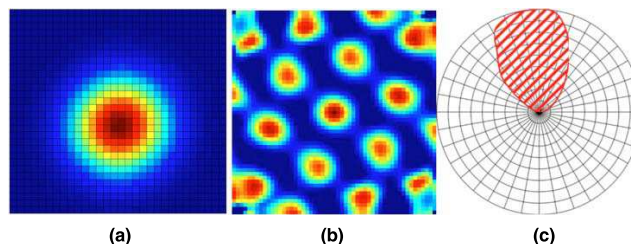Corresponding author: Aura Ganz (e-mail: ganz@ umass.edu).

Fig. 1. Illustration of firing patterns. In (a) and (b) the color code demonstrates the rate of firing: red shows high activity and blue shows low activity. (a) Place cells (b) Grid cells (c) Head-direction cells

as the cell's 'place field'. Such place fields are considered to be allocentric, implying that they are defined by the external recognizable cues in the environment, for instance, landmarks. While visual input comprises a key element in the formation of place fields, it was shown in [8] that in the absence of visual input, both humans and other vertebrates studied in this context, are capable of generating very effective spatial representations using other sensory input. To strengthen the sensing ability of the BVI user, the proposed framework determines user's location. Moreover, the sensory cues associated with the specific location can be extracted and provided to the BVI user through PERCEPT system.

2. **Grid cells (Fig. 1b)** are neurons within the medial entorhinal cortex (MEC) which exhibit firing at multiple

locations in the environment. The spatial firing fields are positioned regularly in a grid across the environment comprised of equilateral triangles. Unlike place cells, grid cells seem to be the internal cognitive representation of the external Euclidean space. Moreover, it is found that grid cells play a critical role in path integration (i.e. navigation or wayfinding) since their firing depends on the ego-motion of the individuals, such as moving direction.

3. **Border/boundary vector cells** are neurons found in the hippocampal formation which fire when the individual is at a specific distance and direction relative to the environment boundaries such as walls, low ridges or vertical drops. The landmark proximity function in the proposed sensing framework enables PERCEPT to alert the user about these environment boundaries.

4. **Head-direction cells (Fig. 1c)** are neurons which fire maximally when an animal's head faces a particular direction in the azimuthal (horizontal) plane. The firing relies on the angular position of environmental cues [9-12]. Like place cells, the firing of head direction cells has been shown to rely on the angular position of environmental cues and generate a lobe of a certain width. The sensing framework estimates the

Fig. 2. PERCEPT system architecture

Fig. 3. Sensing framework overview
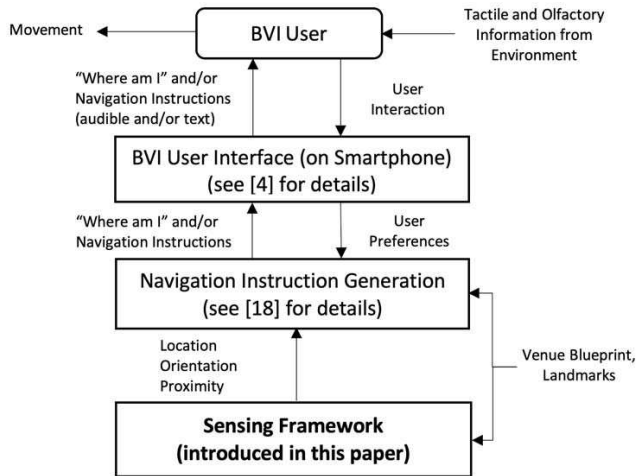
user moving direction which enables PERCEPT to provide directional instructions to the BVI user.

These extraordinary findings that confirm the spatial nature of the entorhinal-hippocampal system led to the award of the 2014 Nobel Prize in Physiology or Medicine to O'Keefe and the Mosers for their discovery of "a positioning system in the brain." [13].

It is important to mention that researchers [14-17] have shown that the hippocampus can use non-visuospatial input such as spatial olfactory and tactile information, to generate spatial representations. In spite of the fact that olfactory input is less precise than visual input, it can substitute for visual inputs to enable the acquisition of metric information about space. However, for BVI users traveling through large public venues it is difficult or sometime impossible to use only olfactory and/or tactile information to form the cognitive map of the space. PERCEPT system complements these senses and helps the BVI user to build the cognitive map which helps them independently navigate through large public venues. PERCEPT provides users with audio/text information about their location in space relative to landmarks, proximity to landmarks as well as detailed instructions to their chosen destination. In order to provide such information, PERCEPT system incorporates the sensing framework introduced in this paper. As reported later in this paper, the framework was tested within the entire PERCEPT system and shown that it provides the necessary information that helps BVI users build a cognitive map of the space and reach the chosen destination independently [4]. Fig. 2 illustrates the architecture of PERCEPT system which includes the sensing framework presented in this paper, the navigation and instruction generation module and the user interface.

The sensing framework introduced in this paper includes the following modules that correspond to the abovementioned place, border and head-direction cells: a localization module, a moving direction estimation module and a landmark proximity detection module. Grid cells correspond to the graph representation of space included in the Navigation Instruction Generation Module (see Fig. 2) [18]. As shown in Fig. 3, the
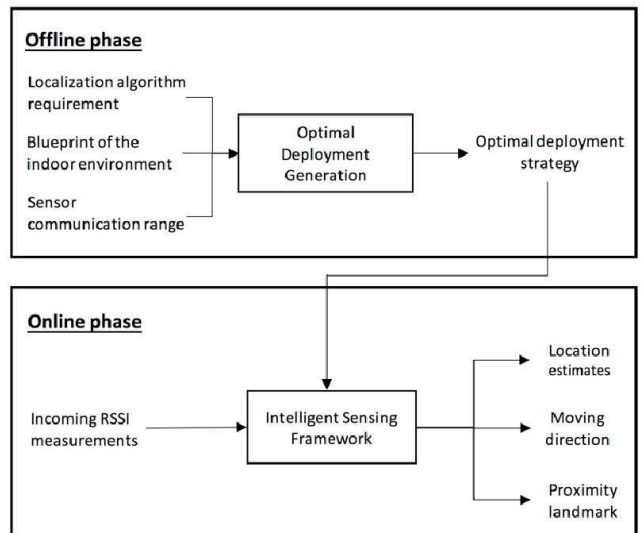
TABLE I
ANALOGY BETWEEN NEURAL REPRESENTATION OF SPACE AND PROPOSED FRAMEWORK

Neuron Type	Neuron Firing Condition given Environment Input	Technical Equivalence (modules) in Sensing Framework (synthesizing input)
Place cells	Fired in small specific regions of the environment	Localization module
Border cells	Fired in small regions around the environment boundary	Landmark proximity detection module (provides border detection as well as proximity to other landmarks)
Head-direction cells	Fired in a range around the head direction	Moving direction module

proposed framework includes two phases, the

offline phase and the online phase. In the offline phase, we generate the optimal sensor deployment strategy for the indoor space, minimizing the cost of the deployment while considering the requirements of the localization algorithm. During the online phase, we develop intelligent sensing algorithms that provide location estimates, moving direction estimates and detect landmarks next to the user. To the best of our knowledge, this is the first comprehensive BLE-based sensing solution that can determine location, moving direction and landmark proximity using only RSSI values. In addition, to make our sensing solution scalable and practical to different spaces, we have introduced an algorithm to determine the sensors' locations in the indoor environment.

Table I summarizes the spatial information represented in each type of neuron and the corresponding modules provided in our framework.

In contrast to the established literature, our framework will not seek to achieve the exact coordinates (e.g. singular point) of the user location or exact value of user orientation in

degrees. Neuroscience reveals that the human cognitive system for positioning and navigation uses a *region* to understand the location instead of a singular point. Therefore, we propose to evaluate the performance of the localization algorithm using the success rate of region detection for different region sizes. In addition, as shown in Fig. 1c and reported in [19], head-direction cells fire in a *range* around the preferred firing direction (e.g. the direction at which neurons fire maximally). Thus, instead of evaluating the moving direction algorithm using deviation of the estimated moving direction from the ground truth, we evaluate its performance using success rate of estimating a 4-way or 8-way cardinal directions.

The remainder of the paper is organized as follows. Section II discusses the related work. The offline phase which includes the optimal deployment strategy generation is introduced in Section III. The online phase which includes localization, moving direction estimation and landmark proximity detection is detailed in Section IV. Experimental results are shown in Section V and Section VI concludes the paper.

II. RELATED WORK

With the advent of smartphones and sensors, indoor localization techniques using Bluetooth Low Energy (BLE) technology have attracted significant interest. In this section, we will present an overview of recent advances in the development of BLE-based indoor localization techniques followed by a discussion of the advantages of the proposed framework over other BLE-based indoor navigation systems for BVI users.

A. Indoor Localization

Using multilateration [20], we can determine the location of the target from the distances between the target and the beacons using the least square algorithm. Given the RSSI, we can derive the distance between the target and the beacon using a prebuilt propagation model. To compensate for the inaccuracy of deriving distance from the propagation model, the authors in [21] perform additional signal processing of the RSSI values and propose to auto-calibrate the propagation model with respect to environmental textures. In [22], the authors present an approach similar to trilateration, named inter Ring Localization Algorithm (iRingLA). Instead of treating the communication range of the transmitter as a circle, iRingLA regards it as a ring and determines the target's location from the intersection of three rings. In [23], the authors try to improve the localization accuracy by applying several techniques. First, instead of using one propagation model for all beacons, they build a propagation model for each beacon. Second, the authors take advantages of Gaussian filtering and other smoothing approaches to reduce the fluctuations of noisy RSSI measurements.

As the least computational expensive approach among all methodologies, proximity algorithms can locate a target using the approximate communication range of a beacon to detect whether the target is in range or not. One of the most popular methods in proximity algorithms is Min-Max approach [20], which aims to find the intersection region from beacons'

communication ranges. In [24] the authors present a two-level localization approach, including low-precision and high-precision indoor localization components. The main idea is to find the intersection region of the beacons using the beacons' different transmission power levels. In [25] the authors combine the stigmergic marking approach with the Min-Max algorithm and draw the location estimation from the stigmergic map. Two other BLE-based approaches [26, 27] adopt the same idea of deriving the location using the beacon with the strongest RSSI value.

Fingerprinting-based algorithms typically contain two phases, the offline training phase and the online localization phase [20]. During the offline phase, the fingerprint data is collected at each reference point in space and then stored in the database. In the online phase, given an RSSI vector collected by a target at a certain point, the algorithm derives the target's location from the location of the reference point at which the fingerprint is most similar to the given RSSI vector using K-nearest neighbors (KNN) algorithm. In [28] the authors utilize the autoencoder, an unsupervised learning algorithm as the denoising function for raw RSSI values. In [29] the authors exploit the Kendall Tau Correlation Coefficient to generate the weights and integrate it into the fingerprinting algorithm. In [30] the authors present an iterative approach for localizing the target by selecting different beacons to obtain RSSI in each iteration and then averaging the location estimations.

Even though fingerprinting-based algorithm can effectively alleviate the negative effect of localizing targets from noisy RSSI measurements to a certain degree, the time-consuming preparation procedure makes it an impractical solution. Thus, some researchers started to work on a more flexible and computation-efficient approach, called Weighted Centroid Localization (WCL). In [31] the authors utilize a Kalman filter to derive the weights for each nearby beacon and then calculate the target's location from the generated weights. In [32] the authors leverage a self-defined propagation model to compute the weights and perform a comprehensive performance comparison between BLE and Wireless Local Area Networks (WLAN) at 2.4GHz and 5GHz. They show that BLE outperforms WLAN in terms of the localization performance using WCL. In our work, we utilize RSSI directly without applying any sophisticated smoothing methods [33]. We compute the weights using the Weighted Path Loss Localization (WPLL) algorithm [35].

B. Indoor Navigation Systems for BVI

Different types of indoor navigation systems have been designed and implemented to make indoor spaces more accessible to BVI users. Such systems use different localizations schemes such as vision-based systems [36-41] wireless-based systems [42-47] and hybrid systems [48-54]. Here, we elaborate on BLE-based systems and compare them with the proposed framework.

A system called NavCog [42] uses a BLE-based localization scheme and was tested by 6 BVI subjects. A fingerprint-based algorithm is used to compute the user's location and the Smartphone compass is used to determine the user's orientation.

They reported several interesting conclusions obtained from users' feedback. One of them is that the precision of the localization algorithm is not a concern as long as the system can help them recover from mistakes quickly.

A hybrid indoor navigation system for BVI users using BLE and Google Tango is proposed in [48]. Authors implemented a two-level localization strategy. At the first level, the RSSI fingerprints are used to find the coarse location of the user and builds an Area Description File (ADF), i.e. a feature map of the space, built by Google Tango. Given the ADF, the software and hardware on Google Tango can localize users with high accuracy. Unfortunately, Google Tango phone was discontinued.

A wayfinding system for large indoor spaces, which is named GuideBeacon, was introduced in [43]. The system can localize the user using a proximity algorithm, which identifies the closest beacon using thresholds. Similar to [42], the directional information is determined by the compass. In [44] the authors propose a localization method that uses the user proximity to a beacon. It is well known that the localization accuracy of the beacon proximity approach depends on the density of the beacons. High beacon density will increase the deployment and maintenance cost.

Unlike prior works in which the BLE sensors' RSSI is used to determine only the user location, our framework provides the user location, orientation and landmark proximity. Our approach does not require any specialized hardware and/or software (e.g. Tango platform) since the user can run the algorithm in any Smartphone. It is important to mention that compass based approaches to determine the user orientation in indoor spaces is very unreliable in areas with strong and changing magnetic fields such as areas near elevators and subway platforms with frequent arrivals of trains. Moreover, to make our solution scalable, we have introduced a systematic way of planning sensor deployment in indoor environments, which is not covered by prior works [42-47]. In addition, we introduce a novel way to evaluate the localization performance which is zone localization, inspired by space encoding in the human brain.

III. OFFLINE PHASE

In this phase we generate an optimal sensor deployment strategy for an indoor environment. The input includes: the blueprint and its associated scale, the sensor communication range and the number of sensors, k, that should cover each point in the blueprint (k is determined by the localization algorithm). To ensure coverage, we use the optimal deployment pattern that guarantees k-covering [55]. If k equals to 3, the optimal deployed pattern is shown in Fig. 4.

The sensor deployment algorithm is implemented in Matlab. The graphical user interface (GUI) which is shown in Fig. 5 includes:

- *Blueprint (Top):* displays the blueprint as background and the superimposed locations of the sensors obtained from the deployment algorithm using red dots.
- *Parameter settings (Input-bottom left):* includes the number of sensors, k, that should cover each point in the
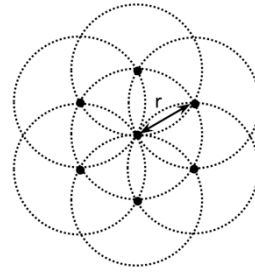

Fig. 4. Optimal pattern when k=3 (r is BLE communication range in ft.)
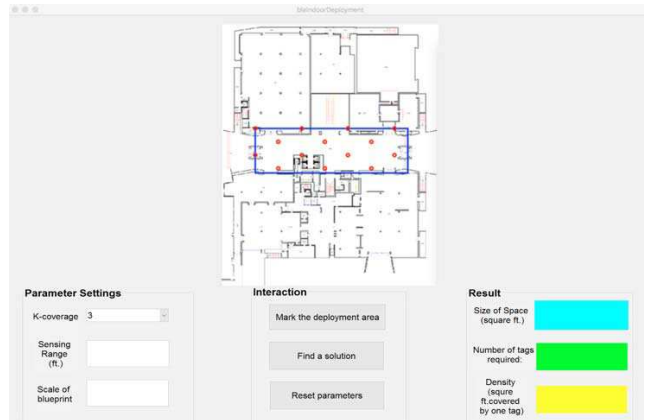

Fig. 5. GUI of the optimal deployment strategy generation

blueprint, the BLE communication range and the scale of the blueprint.
- *Interaction (center):* marks the deployment area with a blue box, triggers the action of computing the optimal deployment or resets the current parameters.
- *Results (Output-bottom right):* the size of the entire area, the total number of beacons required and the density which is defined as the size of area covered by one beacon.

Note that the generated optimal sensor deployment may not be followed exactly while deploying the sensors in the environment due to the physical limitations of each suggested location. Nevertheless, the optimal deployment strategy provides valuable guidelines for guaranteeing the performance of the localization algorithm across the entire environment.

IV. ONLINE PHASE

The online phase includes the following modules: localization (Section IV.A), moving direction estimation (Section IV.B), and landmark proximity detection (Section IV.C).

A. Localization

We assume that the user's smartphone can collect RSSI measurements from k nearby BLE sensors simultaneously. Distance d_i from BLE sensor i to user's smartphone is given by:
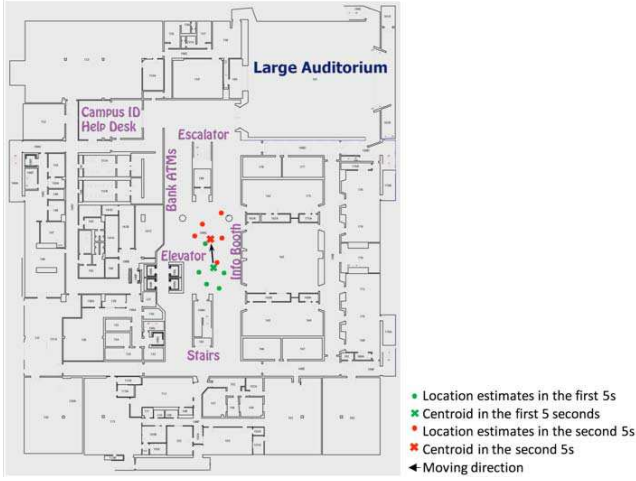
$$d_i = 10^{\frac{s_i - PL_0}{10 * \gamma}} \tag{1}$$

Fig. 6. Illustration of moving direction estimation

TABLE II
PSEUDOCODE OF MOVING DIRECTION ESTIMATION

Input: $N = 10$ seconds (size of the sliding window)
$E = \{\}$ (set of entities to be clustered)
$k = 2$ (number of clusters)
$MaxIters = 300$

Output: $C = \{c_{past}, c_{present}\}$ (set of start and the end of the moving trajectory)

Do the following forever:
if a new location estimate e_i is received, **then**
    add e_i into E
end
if E contains more than N elements, **then**
    foreach $c_i \in C$ **do**
        $c_i \leftarrow e_j \in E$ (e.g. random selection)
    end
    foreach $e_i \in E$ **do**
        $l(e_i) \leftarrow argminDistance(\, e_i, c_j) \, j \in \{1 \ldots k\}$ (e.g. Euclidean distance)
    end

    $changed \leftarrow false$;
    $iter \leftarrow 0$;
    repeat
        foreach $c_i \in C$ **do**
            $updateCluster(c_i)$;
        end
        foreach $e_i \in E$ **do**
            $minDist \leftarrow argminDistance(e_i, c_j) \; j \in \{1 \ldots k\}$;
            if $minDist \neq l(e_i)$ **then**
                $l(e_i) \leftarrow minDist$;
                $changed \leftarrow true$;
            end
        end
        $iter$++;
    until $changed = true$ and $iter \leq MaxIters$;

    $c_{previous} \leftarrow findMostCommonLabel(\{l(e)|e = 1, 2, \ldots, 5\})$;
    $c_{present} \leftarrow findMostCommonLabel(\{l(e)|e = 6, 7, \ldots, 10\})$;
    $C = \{c_{previous}, c_{present}\}$;
end

where s_i is the RSSI collected from BLE sensor i, γ is the path loss component and PL_0 is the path loss at the reference distance d_0.

Equation (2) describes the Log-distance path loss propagation model. Given a certain *distance*, d_i, s_i can be computed by:

$$s_i = PL_0 + 10 * \gamma * \log_{10}(d_i/d_0) \tag{2}$$

The weighting factor w_i is given by:

$$w_i = \frac{1/d_i}{\sum_{i=1}^{k} 1/d_i} \tag{3}$$

The location estimate (u, v) of the user can be obtained by:

$$u = \sum_{i=1}^{k} w_i * x_i \tag{4}$$

$$v = \sum_{i=1}^{k} w_i * y_i \tag{5}$$

where (x_i, y_i) is the 2D location of BLE sensor i.

B. Moving Direction Estimation

To determine user's moving direction from the sequence of location estimations, we use the K-means clustering algorithm in conjunction with a sliding time window.

Given a set of location estimates computed in the past N seconds, $e^{(1)} \ldots, e^{(N)}$, we group the data into two cohesive clusters, extracting the moving trajectory from two centroids. The pseudocode implementation of the algorithm is provided in Table II.

As shown in Fig. 6, we cluster the location estimates in a time window into two groups using K-means algorithm. Using the centroids of the two clusters, we determine the moving direction by finding the trajectory from the past centroid to the present one.

C. Landmark Proximity Detection

In addition to location and moving direction estimation, the proposed framework also offers the functionality of landmark proximity detection which can helps the user build the cognitive map of the space.

We define a proximity radius for each landmark. Since our detection problem can be treated as a binary classification problem, we leverage the naïve Bayes classifier to detect a landmark next to the user. For each landmark, the two possible outcomes are either the user location is in close proximity to the landmark (i.e. within the proximity radius of the landmark) or not (i.e., the user location is out of of the proximity radius of the landmark). We train the probabilistic model that will be used in naïve Bayes classifier using the RSSI measurements collected at different distances. For the labelling process, all the RSSI measurements collected within the radius are labelled with 1, and other measurements are labelled with 0.

Mathematically, the conditional probability model for each landmark can be calculated using (6).

$$p\left(C_i^k | x_i^1, \ldots x_i^n\right) \propto p(C_i^k, x_i^1, \ldots x_i^n) \tag{6}$$

where x_i^j denotes the j th RSSI measurement from sensor i, and C_i^k refers to class k for landmark i (each landmark is paired with a certain sensor) with $k = 1$ (we are in the proximity of landmark k), $k = 0$ otherwise.

The joint model can be expressed as follows:

$$p\left(C_i^k, x_i^1, \ldots x_i^n\right)$$
$$= p\left(C_i^k\right) p\left(x_i^1 | C_i^k\right) p\left(x_i^2 | C_i^k\right) \ldots$$
$$= p(C_i^k) \prod_{j=1}^{n} p(x_i^j | C_i^k) \qquad (7)$$

Finally, the decision can be made using:

$$\hat{y}_i = arg \max_{k \in \{0,1\}} p(C_i^k) \prod_{j=1}^{n} p(x_i^j | C_i^k) \qquad (8)$$

where n refers to the number of RSSI measurements collected from the sensor that is paired with landmark i, $\hat{y}_i$ denotes the estimated class for landmark i.

V. EXPERIMENTAL RESULTS

To evaluate the performance of the algorithms included in the proposed framework, we deployed our testbed at the basement level of UMass Campus Center, which is a 9,000 ft^2 area (see Fig. 7). We use BLE sensors manufactured by Kontact.io and different models of iPhones (iPhone 6, iPhone 6 plus and iPhone 6s plus). The hardware specifications [56] of the BLE sensor are provided in Table III. The sensors' transmission power is set to medium level, -12 dBm. Due to the default Bluetooth communication setting in iOS, the frequency of collecting the RSSI signal is 1 Hz. The BLE sensors are deployed following the guidelines provided by the optimal deployment strategy with minor adjustment to the environment.

Our dataset contains 35 and 34 groups of RSSI measurements along Route 1 and Route 2, respectively. On each route that takes about 1-2 minutes from start to end, we collect about 100 location estimates. With nearly 7,000 location estimations calculated in total, over a thousand orientation and landmark proximity estimates are computed. As shown in Fig. 7, we collected RSSI measurements following the testing routes so that the ground truth walking trajectory is known to us. Along each route, we pressed a button on our data collection application when we passed by the marked checkpoints (6 for Route 1 and 4 for Route 2). The

recorded information is used as the ground truth for evaluating the proximity landmark detection module. Since we also know that the moving direction for each walking trajectory, the ground truth moving direction can be collected as well.

A. Localization

In equations introduced in Section IV.A we use $PL_0 = -63.5379$ dB, $\gamma = -2.086$ and $d_0 = 3$ft. These parameters in (2) are calculated by solving the nonlinear regression problem of the pre-collected data at different sampling points between 3 ft and 45 ft at 3ft intervals. We collected 200 readings at each sampling point.

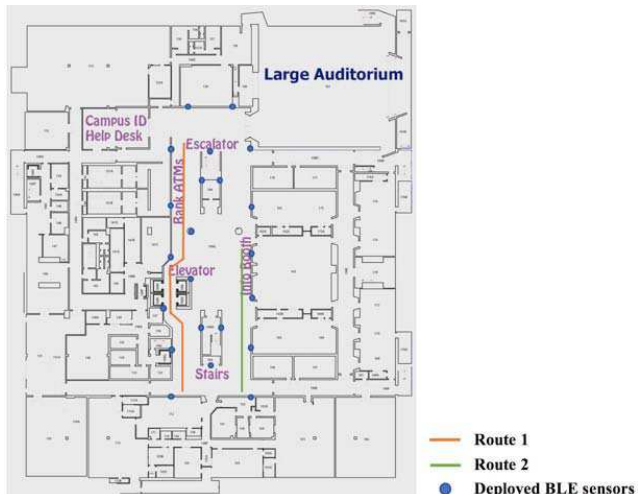| Model	Tough Beacon
Operating Frequency	2.4 GHz
Transmission Power	-30 dBm to 4 dBm
Transmission Range	Up to 100 ft.
Time Interval	350 ms
Battery Life	Up to 2 years with default setting

Fig. 7. Testbed at UMass campus center (180 ft. x 50 ft.)

We evaluate the success rate of region detection which is defined as the ratio between the number of correct region estimations over the total number of region estimations (correct and incorrect). The choice of region localization is inspired by the spatial representation in cognitive neuroscience [6]. As detailed above, the human cognitive system for positioning and navigation uses a region to understand the location instead of a singular point. As shown in Fig. 8, we generate the hexagon tessellation of the space following the format of spatial representation used in neural cells [6]. As we learned from cognitive neuroscience, grid cells fire in a certain pattern (see the Fig. 9a). If we connect the centers of the firing regions, it can cover the entire space with equilateral triangles. As shown in Fig. 9b, we connected the centroids of the neighboring equilateral triangles of a certain region, which form a hexagon pattern. It turns out this is the best tessellation pattern that determines regions used to evaluate the accuracy of the proposed localization algorithm. As shown in Fig. 10, while the radius of the hexagon-shaped region increases from 10 ft. to 20 ft., the success rate of region detection increases from 62.5% to 83%.

B. Moving Direction Estimation

According to a neuroscientific study reported in [19], the head-direction cells used in human cognitive system for orientation will fire in a *range* around the preferred firing direction
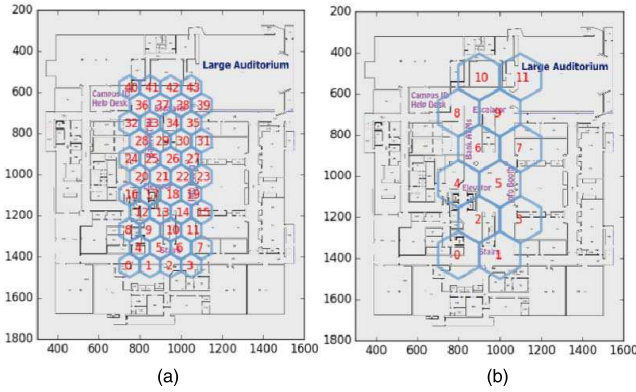
Fig. 8. Hexagon tessellation of the space (a) Radius is 10 ft. (b) Radius is 20 ft.
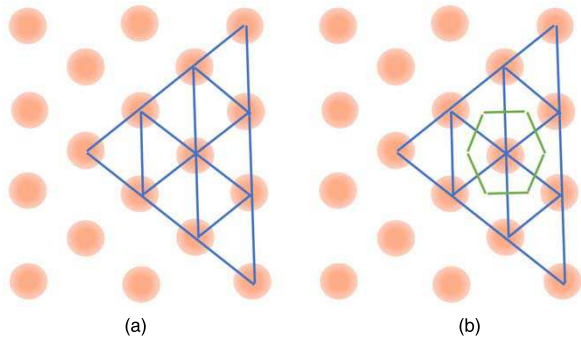

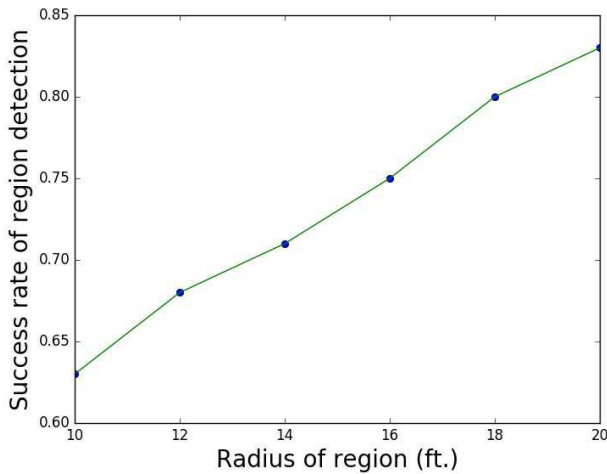Fig. 9. Grid cell firing pattern in (a) and Hexagon formation in (b)

Fig. 10. Experimental results of region detection

which is defined as the direction at which the neuron fires maximally. Thus, to evaluate the moving direction module, we propose to evaluate the success rate of estimating a specific cardinal direction (see Fig. 11) determined by the orientation vector calculated in Section IV.B. Using a 10-second sliding window, 1395 estimates are generated by our dataset.

Among these estimates, the orientation estimation success rates for 4-way and 8-way cardinal directions are about 94% and 60 %, respectively.
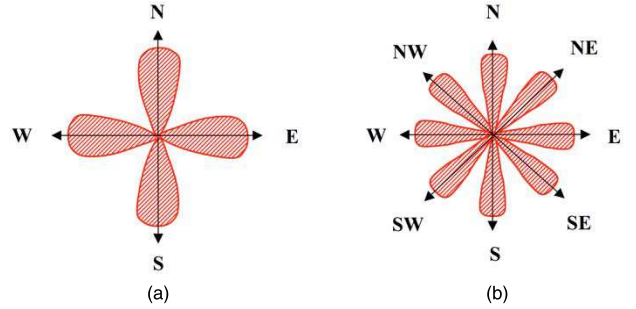

Fig. 11. Illustration of Head-direction cells firing pattern around cardinal directions (a) 4-way cardinal directions (b) 8-way cardinal directions

C. Landmark Proximity Detection

The success rate of landmark proximity detection is defined as the ratio between the number of correct proximity landmark detections over the total number of proximity landmark detections (correct and incorrect). Using a 6-ft. proximity radius around each landmark, and 1153 estimates, we obtain a landmark proximity detection success rate of 81%.

D. Integration With Percept Indoor Navigation System for BVI Users

The proposed sensing framework was integrated in PERCEPT system (see Fig. 2) and tested in a large public transportation hub in Boston [4]. Using PERCEPT application installed on users' iPhones, BVI users can: 1) understand where they are in space audibly using regions and moving direction calculated by our sensing framework, 2) receive audible navigation instructions from one landmark to another using surrounding landmarks, and 3) receive alerts if they approach some landmarks via proximity landmark detection.

The system has been tested by 6 BVI subjects in a subway station [4]. The experiments show that the users can successfully and independently reach their chosen destinations. All participants were very satisfied with the navigational aid provided by PERCEPT. Details of this deployment as well as testing results can be found in [4].

It is important to note that we expect that the user will make mistakes (i.e., reach wrong landmarks or just get disoriented in the environment) and therefore require rerouting. Rerouting assistance in the application includes the ability to press "Where am I" as well as provide instructions from any landmark to the chosen destination. It was interesting to observe that the participants reported that they have built a cognitive map of the environment using the application routing and rerouting features as well as the "Where am I" feature.

For completeness of the paper we include some of the feedback provided by the BVI users which participated in these trials. We collected the participants' feedback using a

qualitative questionnaire. Each participant was asked to score their agreement with specific statements related to their experience during the trial. The score followed Likert scale from 1 strongly disagree to 7 strongly agree with, with 4 being neither agreeing or disagreeing with the statement. The average scores are provided in Table IV. The nine additional

TABLE IV
POST-TRIAL QUESTIONNAIRE USING LIKERT SCALE SCORE

Statements	Average Score
Easy to learn how to use system	6.7
Easy to use the system	6.7
Trial design was easy to complete	6.3
Easy to use User Interface	6.5
System provided sufficient re-orientation information when lost	5.5
I am confident I will reach the destination using this system	6.7

trials we performed in a large indoor transportation venue showed similar trends.

As shown above, we conclude that the information we compute in the proposed sensing framework, i.e., zone localization, region orientation and proximity, can be successfully used by the navigation instructions module to convey the necessary information to allow the BVI user to independently navigate through large indoor venues.

VI. CONCLUSIONS

In this paper, we introduced a sensing framework that includes optimal deployment strategy, location estimation, moving direction estimation and landmark proximity detection. We note that in spite of the fact that the location, orientation and proximity results computed by our sensing framework are not accurate, they provide the necessary information to the rest of PERCEPT modules and ultimately enable the BVI user to successfully navigate independently in large indoor venues. It is interesting to note that unlike a sensing framework for robots that needs to provide very accurate location and orientation, in the proposed framework used by BVI users high accuracy is not necessary. The reason is that the movement/navigation decisions made by the user include diverse aspects such as how the navigation instructions are composed, how the user interface is designed and how accurate the user can interpret the instructions and/or manipulate the user interface. Our observation is also aligned with the space encoding methods presented in this paper which show that the brain encodes zones (place fields) using place cells (i.e., zones, not singular points) as well as orientation regions using head cells with wide lobes (see Fig. 1c) (i.e., do not record highly accurate directions using very narrow width lobe).

REFERENCES

[1] "Statistical Snapshots from the American Foundation for the Blind," Assessment Considerations for Students who are Blind and Visually Impaired - American Foundation for the Blind. [Online]. Available: http://www.afb.org/info/blindness-statistics/2. [Accessed: 20-Aug-2018].

[2] A. Ganz *et al*, "PERCEPT: Indoor navigation for the blind and visually impaired," in *Engineering in Medicine and Biology Society, EMBC, 2011 Annual International Conference of the IEEE*, 2011, pp. 856-859.

[3] A. Ganz *et al*, "PERCEPT-II: Smartphone based indoor navigation system for the blind," in *Engineering in Medicine and Biology Society (EMBC), 2014 36th Annual International Conference of the IEEE*, 2014, pp. 3662-3665.

[4] A. Ganz *et al*, "PERCEPT Navigation for Visually Impaired in Large Transportation Hubs", *Journal on Technology and Persons with Disabilities*, vol. 6, pp. 336-353, 2018.

[5] R. A. Epstein *et al*, "The cognitive map in humans: spatial navigation and beyond," *Nat. Neurosci.,* vol. 20, *(11)*, pp. 1504, 2017.

[6] M. B. Moser, D. C. Rowland and E. I. Moser, "Place cells, grid cells, and memory," *Cold Spring Harb Perspect. Biol.,* vol. 7, *(2)*, pp. a021808, Feb 2, 2015.

[7] J. O'Keefe, "Place units in the hippocampus of the freely moving rat," *Exp. Neurol.,* vol. 51, *(1),* pp. 78-109, 1976.

[8] V. R. Schinazi, T. Thrash and D. Chebat, "Spatial navigation by congenitally blind individuals," *Wiley Interdisciplinary Reviews: Cognitive Science,* vol. 7, *(1),* pp. 37-58, 2016.

[9] J. P. Goodridge and J. S. Taube, "Preferential use of the landmark navigational system by head direction cells in rats." *Behav. Neurosci.,* vol. 109, *(1),* pp. 49, 1995.

[10] J. S. Taube, "Head direction cells recorded in the anterior thalamic nuclei of freely moving rats," *J. Neurosci.,* vol. 15, *(1 Pt 1),* pp. 70-86, Jan, 1995.

[11] J. S. Taube, R. U. Muller and J. B. Ranck Jr, "Head-direction cells recorded from the postsubiculum in freely moving rats. I. Description and quantitative analysis," *J. Neurosci.,* vol. 10, *(2),* pp. 420-435, Feb, 1990.

[12] M. B. Zugaro, E. Tabuchi and S. I. Wiener, "Influence of conflicting visual, inertial and substratal cues on head direction cell activity," *Experimental Brain Research,* vol. 133, *(2),* pp. 198-208, 2000.

[13] "The 2014 Nobel Prize in Physiology or Medicine – Press Release," *Nobleprize.org.* [Online]. Available: https://www.nobelprize.org/nobel_prizes/medicine/laureates/2014/press.html. [Accessed: 20-Aug-2018]

[14] E. Save, L. Nerad and B. Poucet, "Contribution of multiple sensory information to place field stability in hippocampal place cells," *Hippocampus,* vol. 10, *(1),* pp. 64-76, 2000.

[15] S. Zhang *et al*, "Spatial representations of place cells in darkness are supported by path integration and border information," *Frontiers in Behavioral Neuroscience,* vol. 8, pp. 222, 2014.

[16] E. J. Markus *et al*, "Spatial information content and reliability of hippocampal CA1 neurons: effects of visual input," *Hippocampus,* vol. 4, *(4),* pp. 410-421, 1994.

[17] G. J. Quirk, R. U. Muller and J. L. Kubie, "The firing of hippocampal place cells in the dark depends on the rat's recent experience," *J. Neurosci.,* vol. 10, *(6),* pp. 2008-2017, Jun, 1990.

[18] Y. Tao, "Scalable and vision free user interface approaches for indoor navigation systems for the visually impaired," M.S. thesis, Dept. Elect. Comput. Eng., Univ. Massachusetts Amherst, Amherst, MA, USA, 2015.

[19] J. Taube, "Head direction cells," *Scholarpedia.* [Online]. Available: http://www.scholarpedia.org/article/Head_direction_cells. [Accessed: 20-Aug-2018].

[20] J. Zhou and J. Shi, "RFID localization algorithms and applications—a review," *J. Intell. Manuf.*, vol. 20, *(6),* pp. 695-707, 2009.

[21] N. Kuxdorf-Alkirata *et al*, "A self-calibrating bidirectional indoor localization system," in *Acoustics, Speech and Signal Processing (ICASSP), 2017 IEEE International Conference on*, 2017, pp. 3276-3280.

[22] A. Thaljaoui *et al*, "BLE localization using RSSI measurements and iRingLA," in *Industrial Technology (ICIT), 2015 IEEE International Conference on*, 2015, pp. 2178-2183.

[23] Z. Jianyong *et al*, "RSSI based bluetooth low energy indoor positioning," in *Indoor Positioning and Indoor Navigation (IPIN), 2014 International Conference on*, 2014, pp. 526-533.

[24] Y. Wang *et al*, "RSSI-based bluetooth indoor localization," in *Moile Ad-Hoc and Sensor Networks (MSN), 2015 11th International Conference on*, 2015, pp. 165-171.

[25] F. Palumbo *et al*, "A stigmergic approach to indoor localization using bluetooth low energy beacons," in *Advanced Video and Signal Based Surveillance (AVSS), 2015 12th IEEE International Conference on*, 2015, pp. 1-6.

[26] Z. Li, Y. Yang and K. Pahlavan, "Using iBeacon for newborns localization in hospitals," in *Medical Information and Communication Technology (ISMICT), 2016 10th International Symposium on*, 2016, pp. 1-5.

[27] S. Alletto *et al*, "An indoor location-aware system for an IoT-based smart museum," *IEEE Internet of Things Journal*, vol. 3, *(2),* pp. 244-253, 2016.

[28] C. Xiao *et al*, "3D BLE Indoor Localization based on Denoising Autoencoder," *IEEE Access*, vol. 5, pp. 12751-12760, 2017.

[29] Z. Ma *et al*, "A BLE RSSI ranking based indoor positioning system for generic smartphones," in *Wireless Telecommunications Symposium (WTS), 2017*, 2017, pp. 1-8.

[30] Y. Peng *et al*, "An iterative weighted KNN (IW-KNN) based indoor localization method in bluetooth low energy (BLE) environment," in *Ubiquitous Intelligence & Computing, Advanced and Trusted Computing, Scalable Computing and Communications, Cloud and Big Data Computing, Internet of People, and Smart World Congress (UIC/ATC/ScalCom/CBDCom/IoP/SmartWorld), 2016 Intl IEEE Conferences,* 2016, pp. 794-800.

[31] S. Subedi *et al*, "Beacon based indoor positioning system using weighted centroid localization approach," in *Ubiquitous and Future Networks (ICUFN), 2016 Eighth International Conference on*, 2016, pp. 1016-1019.

[32] E. S. Lohan *et al*, "Received signal strength models for WLAN and BLE-based indoor positioning in multi-floor buildings," in *Localization and GNSS (ICL-GNSS), 2015 International Conference on*, 2015, pp. 1-6.

[33] D. Ordóñez-Camacho and E. Cabrera-Goyes, "An adaptive-bounds band-pass moving-average filter to increase precision on distance estimation from bluetooth RSSI," in *International Conference on Information Theoretic Security,* 2018, pp. 823-832.

[34] "Log-distance path loss model," Wikipedia, 03-Jul-2018. [Online]. Available: https://en.wikipedia.org/wiki/Log-distance_path_loss_model. [Accessed: 20-Aug-2018].

[35] H. Zou *et al*, "An RFID indoor positioning system by using weighted path loss and extreme learning machine," in *Cyber-Physical Systems, Networks, and Applications (CPSNA), 2013 IEEE 1st International Conference on*, 2013, pp. 66-71.

[36] H. Wang *et al*, "Enabling independent navigation for visually impaired people through a wearable vision-based feedback system," in *2017 IEEE International Conference on Robotics and Automation (ICRA),* 2017, pp. 6533-6540.

[37] G. Garcia and A. Nahapetian, "Wearable computing for image-based indoor navigation of the visually impaired," in *Proceedings of the Conference on Wireless Health,* 2015, pp. 17.

[38] Z. Yang and A. Ganz, "Egocentric landmark-based indoor guidance system for the visually impaired," in *Computer Vision: Concepts, Methodologies, Tools, and Applications,* IGI Global, 2018, pp. 1483-1499.

[39] B. Li *et al*, "Vision-based Mobile Indoor Assistive Navigation Aid for Blind People," *IEEE Transactions on Mobile Computing,* pp. 1-1, 2018.

[40] G. E. Legge *et al*, "Indoor navigation by people with visual impairment using a digital sign system," *PloS One,* vol. 8, *(10),* pp. e76783, 2013.

[41] M. Serrão *et al*, "Indoor localization and navigation for blind persons using visual landmarks and a GIS," *Procedia Computer Science,* vol. 14, pp. 65-73, 2012.

[42] D. Ahmetovic *et al*, "NavCog: A navigational cognitive assistant for the blind," in *Proceedings of the 18th International Conference on Human-Computer Interaction with Mobile Devices and Services,* 2016, pp. 90-99.

[43] S. A. Cheraghi, V. Namboodiri and L. Walker, "GuideBeacon: Beacon-based indoor wayfinding for the blind, visually impaired, and disoriented," in *Pervasive Computing and Communications (PerCom), 2017 IEEE International Conference on,* 2017, pp. 121-130.

[44] S. Bilgi, O. Ozturk and A. G. Gulnerman, "Navigation system for blind, hearing and visually impaired people in ITU ayazaga campus," in *Computing Networking and Informatics (ICCNI), 2017 International Conference on,* 2017, pp. 1-5.

[45] K. Liu, X. Liu and X. Li, "Guoguo: Enabling fine-grained smartphone localization via acoustic anchors," *IEEE Transactions on Mobile Computing,* vol. 15, *(5),*pp. 1144-1156, 2016.

[46] A. Kassim *et al*, "Indoor Navigation System based on Passive RFID Transponder with Digital Compass for Visually Impaired People," *International Journal of Advanced Computer Science and Applications,* vol. 7, *(2),* pp. 604-611, 2016.

[47] A. S. Martinez-Sala *et al*, "Design, implementation and evaluation of an indoor navigation system for visually impaired people," *Sensors,* vol. 15, *(12),* pp. 32168-32187, 2015.

[48] V. Nair *et al*, "A Hybrid Indoor Positioning System for the Blind and Visually Impaired Using Bluetooth and Google Tango," *Journal on Technology and Persons with Disabilities,* vol. 6, pp. 61-81, 2018.

[49] A. Meliones and D. Sampson, "Blind MuseumTourer: A System for Self-Guided Tours in Museums and Blind Indoor Navigation," *Technologies,* vol. 6, *(1),* pp. 4, 2018.

[50] G. Galioto *et al*, "Sensor fusion localization and navigation for visually impaired people," in *Proceedings of the 23rd Annual International Conference on Mobile Computing and Networking,* 2017, pp. 471-473.

[51] M. Murata *et al*, "Smartphone-based indoor localization for blind navigation across building complexes," in *2018 IEEE International Conference on Pervasive Computing and Communications (PerCom),* 2018, pp. 1-10.

[52] J. P. Gomes*et al*, "An indoor navigation architecture using variable data sources for blind and visually impaired persons," in *2018 13th Iberian Conference on Information Systems and Technologies (CISTI),* 2018, pp. 1-5.

[53] R. K. Katzschmann, B. Araki and D. Rus, "Safe Local Navigation for Visually Impaired Users With a Time-of-Flight and Haptic Feedback Device," *IEEE Transactions on Neural Systems and Rehabilitation Engineering,*vol. 26, *(3),* pp. 583-593, 2018.

[54] L. A. Guerrero, F. Vasquez and S. F. Ochoa, "An indoor navigation system for the visually impaired," *Sensors,* vol. 12, *(6),* pp. 8236-8258, 2012.

[55] W. Ku, K. Sakai and M. Sun, "The optimal k-covering tag deployment for RFID-based localization," *Journal of Network and Computer Applications*, vol. 34, *(3),* pp. 914-924, 2011.

[56] "Tough Beacon," Double Battery. [Online]. Available: https://store.kontakt.io/our-products/28-tough-beacon.html. [Accessed: 20-Aug-2018].

ZHUORUI YANG (S'18) received the B.Eng. degree in Electronic and Information Engineering from the Kunming University of Science and Technology, China, M.Sc. degree and Ph.D. degree in Electrical and Computer Engineering from the University of Massachusetts Amherst, USA.

From 2012 to 2018, he has been a Research Assistant in the 5G Mobile Evolution Laboratory, Department of Electrical and Computer Engineering, University of Massachusetts Amherst, USA. His research interests include indoor localization and navigation, computer vision, sensor fusion, machine learning, mobile computing and assistive technologies.

AURA GANZ (M'88-SM'90-F'08) received B.Sc. degree, M. Sc. degree and Ph.D. degree in computer science from Technion, Haifa, Israel.

She is a Professor with the Electrical and Computer Engineering Department and the Director of the 5G Mobile Evolution Laboratory with the University of Massachusetts, Amherst. She has more than 25 years of experience in research, development, implementation and testing of wireless systems as well as systems related to healthcare settings such as assistive technologies for the blind, disaster informatics mobile tele-medicine, and tele-surgery. This work has resulted in more than 250 journal and conference publications in highly respected refereed journals (IEEE, IEE, ACM, Kluwer, Elsevier) with multiple best paper awards. The external recognition of her work is also evidenced by having been selected to serve on leading roles in many professional conferences and workshops as well as being elected as IEEE Fellow. Her research was continuously funded by federal agencies, such as NSF, NIH, ARO, AFOSR, and DARPA, state agencies, such as MassDOT, and industry, such as Microsoft, Intel, and EMC.